Morphology Control for Al_2O_3 Inclusion Without Ca Treatment in High-Aluminum Steel

SHENGPING HE, GUJUN CHEN, YINTAO GUO, BOYI SHEN, and QIAN WANG

Nozzle blockage is a major problem during continuous casting of Al-containing steel. Herein, we analyzed the thermodynamic equilibrium behavior between aluminum and oxygen in steel at 1873 K (1600 °C) and demonstrated that, the dissolved [O] initially decreases with increasing the dissolved [Al] until approximately 0.1 wt pct [Al], and after that, the dissolved [O] increases with dissolved [Al]. Thus, for high-aluminum steel with 1.0 wt pct dissolved [Al], the precipitation of Al_2O_3 inclusion can be avoided during cooling from deoxidation temperature to the liquidus temperature, if the actual dissolved [O] can be kept from increasing when the dissolved [Al] further increases from 0.1 to 1.0 wt pct. Hence, a method of inclusion control for high-aluminum steel without traditional Ca treatment technology was proposed based on the thermodynamic analysis. Industrial tests confirmed that low-melting point Ca-aluminate inclusions were observed typically through a slag washing with SiO_2-minimized high-basicity slag during tapping, accompanied by two-step Al-adding process for production of high-aluminum steel. Moreover, there was no nozzle clogging occurred for five heats of continuous casting.

DOI: 10.1007/s11663-014-0264-z

I. INTRODUCTION

ALUMINUM is usually used for melt deoxidation in the secondary refining of steel owing to its high deoxidation efficiency. Nozzle clogging can occur because of the adherence of solid Al_2O_3 inclusions, formed during deoxidation, to the inner wall of the immersion nozzle. This nozzle clogging can disturb the mold flow, which affects the bloom surface quality, and in extreme cases, the casting sequence can be interrupted.[1–4] Al_2O_3 inclusions in liquid steel can also be absorbed by mold fluxes during continuous casting. Thus, the practical flux may differ significantly from the predetermined flux in terms of its chemical composition and properties. Performance may become worse, ultimately blocking the continuous casting and even cause production accidents.[5,6] To resolve this, calcium treatment is widely used for Al_2O_3 inclusions modification in conventional Al-containing steel ([Al] = 0.02 to 0.06 wt pct) to transform solid Al_2O_3 inclusions into low-melting point Ca-aluminates, which are less harmful to steel properties and increase the castability of steel by minimizing, and ideally eliminating nozzle clogging.[7–10] Numerous theoretical calculations and practical studies have indicated that the required dissolved [Ca] should be proportional to the dissolved [Al] in steel to obtain liquid Ca-aluminates, and the [wt pct Ca]/[wt pct Al] ratio should be controlled at ~0.1.[7,11–15] However, for many high-aluminum steels such as 38CrMoAl, transformation induced plasticity steel (TRIP), and twinning induced plasticity steel (TWIP), the dissolved [Al] is above 0.5 wt pct, indicating that the dissolved [Ca] would need to be 0.05 wt pct, which may exceed the solubility of [Ca] in the molten steel,[8,16] and thus, it may be not feasible to completely transform Al_2O_3 inclusions to liquid Ca-aluminates for high-aluminum steels by calcium treatment. Besides, during the calcium treatment, higher dissolved [Ca] may also react with dissolved [S] to form solid CaS, which may also cause serious nozzle blockage during casting.[7,17–21] Hence, the values of $[\text{wt pct S}]^3 \times [\text{wt pct Al}]^2$ must be controlled below ~0.9×10^{-9} to 5.6×10^{-9} in order to get liquid Ca-aluminates rather than solid CaS at casting temperature [1823 K (1550 °C)],[19,22–24] which implies a maximum allowable [S] of ~9.7 to 17.8 ppm for a steel containing 1.0 wt pct [Al]. Clearly, it is nearly impossible to obtain liquid Ca-aluminates and avoid the formation of solid CaS by calcium treatment for a steel containing 1.0 wt pct [Al].

In this study, the thermodynamics between aluminum and oxygen in liquid steel as well as slag and steel equilibrium was discussed, and industrial trials were performed to develop an alternate process for improving the castability of high-aluminum steel 38CrMoAl without calcium treatment. The proposed process incorporates slag washing with SiO_2-minimized high-basicity slag during tapping, accompanied by two-step Al-adding process and appropriate top-slag refining process, to control the shape of Al_2O_3 inclusions and thereby create favorable conditions to satisfy the requirement of castability for production of high-aluminum steel in the absence of calcium treatment.

SHENGPING HE, Associate Professor, GUJUN CHEN and YINTAO GUO, Ph.D Candidates, BOYI SHEN, Master Candidate, and QIAN WANG, Professor, are with the College of Materials Science and Engineering, Chongqing University, Chongqing 400044, P.R. China. Contact e-mail: heshp@cqu.edu.cn
Manuscript submitted March 1, 2014.
Article published online January 6, 2015.

Table I. Typical Composition of 38CrMoAl Steel (Weight Percent)

C	Si	Mn	Cr	Mo	Al	P	S
0.38	0.30	0.50	1.50	0.18	1.00	0.013	0.002

Table II. First-Order Interaction Coefficients e_i^j at 1873 K (1600 °C)

	j								
i	C	Si	Mn	P	S	O	Al	Cr	Mo
O	−0.450	−0.131	−0.021	0.070	−0.133	−0.2[27]	−3.9[27]	−0.04	0.0035
Al	0.091	0.006	—	—	0.030	−6.6[27]	0.045[27]	—	—
Si	0.18	0.11	0.002	0.11	0.056	−0.23	0.058	−0.0003	—

(Those without citation are taken from Reference[26]).

II. THERMODYNAMICS OF HIGH-ALUMINUM STEEL

A. *Aluminum-Oxygen Equilibrium*

Aluminum deoxidation equilibrium is represented by (Reference 25)

$$(Al_2O_3)_{inclusion} = 2[Al] + 3[O], \quad [1]$$

$$\begin{aligned}\log K_{Al_2O_3} &= \log\left(\frac{a_{Al}^2 \cdot a_O^3}{a_{Al_2O_3}}\right) \\ &= \log\left(\frac{(f_{Al}[\text{pct Al}])^2 \cdot (f_O[\text{pct O}])^3}{a_{Al_2O_3}}\right) \\ &= 20.57 - 64000/T,\end{aligned} \quad [2]$$

where f_i is the activity coefficient of the elemental species i, a_i $(= f_i[\text{wt pct } i])$ is the activity of the species i and can be expressed relative to Henry's law in terms of mass percent owing to the low [Al] and [O] in liquid Fe.

Assuming that solid Al_2O_3 is pure ($a_{Al_2O_3} = 1$), the reaction equilibrium constant $K_{Al_2O_3}$ is

$$\log K_{Al_2O_3} = 2\log f_{Al} + 2\log[\text{pctAl}] + 3\log f_O + 3\log[\text{pctO}]. \quad [3]$$

The dependence of the activity coefficient with the concentration in multicomponent systems is expressed using the solute interaction parameters according to Wagner's formalism.[26]

$$\begin{aligned}\log f_{Al} = &\sum e_{Al}^j[\text{pct}j] + e_{Al}^{Al}[\text{pctAl}] + e_{Al}^{O}[\text{pctO}] \\ &+ r_{Al}^{O}[\text{pctO}]^2 + r_{Al}^{Al,O}[\text{pctAl}][\text{pctO}],\end{aligned} \quad [4]$$

$$\begin{aligned}\log f_O = &\sum e_O^j[\text{pct}j] + e_O^{Al}[\text{pctAl}] + e_O^{O}[\text{pctO}] \\ &+ r_O^{Al}[\text{pctAl}]^2 + r_O^{Al,O}[\text{pctAl}][\text{pctO}],\end{aligned} \quad [5]$$

where j represents the component shown in Table I other than [Al], and e and r are the first- and second-order interaction coefficients, respectively, as shown in Tables II[26] and III.[28]

Table III. Second-Order Interaction Coefficients r_i^j, $r_i^{(i,j)}$ at 1873 K (1600 °C)[28]

r_O^{Al}	r_{Al}^{O}	$r_O^{(Al,O)}$	$r_{Al}^{(Al,O)}$
−0.01	40	47	−0.028

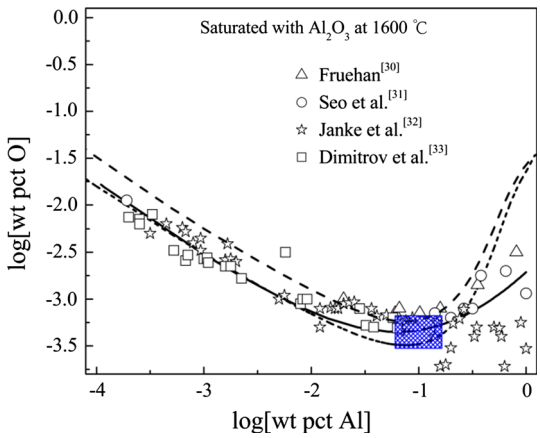

Fig. 1—Dissolved [O] and [Al] of steel in equilibrium with solid Al_2O_3 at 1873 K (1600 °C).

Figure 1 shows the calculated and measured[29–32] relation between the dissolved [O] and [Al] of liquid Fe in equilibrium with solid Al_2O_3 at 1873 K (1600 °C). The solid line and short dashed line were calculated from the associate model[33] and the Wagner's formalism of the systems Fe-Al-O, respectively. Dashed line was also calculated from Wagner formalism, where the elements of steel except Fe, Al, and O belong to 38CrMoAl shown in Table I. It is clear that dissolved [O] decreases with increasing the dissolved [Al] until ~0.07 to 0.1 wt pct [Al], and then dissolved [O] increases with increase in dissolved [Al]. In associate model,[33] the dissolved [Al] and [O] mainly contain associated Al*O as well as unassociated Al and O atoms. At higher dissolved [Al] above the minimum of the deoxidation curve, the Al_2O_3 inclusions can dissolve in the melt again to form associated Al*O, lead to increasing the dissolved [O]. Hence, the equilibrium deoxidation curve

shows a minimum (shadow area), where the dissolved [O] and [Al] are ~3.5 to 4.5 ppm and ~0.07 to 0.1 wt pct, respectively.

When the other alloying elements shown in Table I are taken into account, the equilibrium line (dashed line) moves upward, in which the minimal dissolved [O] is ~5.8 ppm with ~0.08 wt pct dissolved [Al]. Because $K_{Al_2O_3}$ is the equilibrium constant of an endothermic reaction, a decrease in the temperature decreases the equilibrium constant, favoring the precipitation of Al_2O_3 inclusions during the cooling of the liquid steel when dissolved [Al]<0.08 wt pct. However, in the case of higher dissolved [Al] (large than 0.08 wt pct), Al_2O_3 inclusions may not precipitate during cooling if the actual dissolved [O] in liquid steel before cooling can be controlled at the minimum. Figure 2(a) shows the assumed relationship between the dissolved [O] and [Al] in liquid steel at 1873 K (1600 °C), where the solid part of line is calculated from Wagner's formalism, and the dashed part of line is the assumed minimum value (5.8 ppm). Figure 2(b) shows the precipitation of Al_2O_3 inclusions during cooling from the refining temperature [1873 K (1600 °C)] to the liquidus temperature [~1773 K (1500 °C)], where the initial dissolved [O] and [Al] at 1873 K (1600 °C) are assumed to be subordinated to the relation as shown in Figure 2(a). Precipitation of Al_2O_3 inclusions decreases with increasing the initial dissolved [Al], and the precipitation amount can be reduced to zero when initial dissolved [Al] >0.5 wt pct. As we all know, the direct purposes of Ca treatment are transforming the primary Al_2O_3 inclusions generated by deoxidization and second Al_2O_3 inclusions generated during cooling into liquid and globular shaped Ca-aluminate inclusions. In other words, for high-aluminum steels, Ca treatment can be eliminated if the primary Al_2O_3 inclusions can be removed effectively, as well as the Al_2O_3 precipitation can be avoided.

Therefore, based on the above thermodynamic analysis, slag washing during the converter tapping, accompanied with two-step Al-adding process and appropriate top-slag refining process, is proposed as a methodology of Al_2O_3-inclusion control for high-aluminum steel as an alternative to the conventional calcium-wire-feeding process. During the slag washing, an appropriate amount of Al alloys and slagging agents are added to the ladle in the process of tapping and coupled with bottom-argon blowing, the slag-steel interface expands significantly, resulting in a rapid increase in the number of collisions between the inclusions and emulsified slag droplets. Deoxidization products are captured and absorbed by slag droplets, resulting in the modification, floatation, and removal of inclusions.[34] Just as important, in order to controlling the dissolved [O] of molten steel at a minimum, the dissolved [Al] in steel after tapping is strictly limited at 0.08 to 0.12 wt pct. At this moment, the dissolved [O] in steel is only about 5 to 6 ppm. When the slag-washing products are floating and removing as much as possible at the end of LF station, Al alloys are added for the second time to make ~1.0 wt pct dissolved [Al]. At this time, more dissolved [O] is needed to equilibrate with the 1.0 wt pct dissolved [Al] in the liquid steel. However, only a small amount of Al_2O_3 inclusions remain in the liquid steel, so that the re-dissolution amount of Al_2O_3 inclusions can be minimized. As a result, the actual dissolved [O] in liquid steel can be maintained at the minimum when the dissolved [Al] further increases from ~0.1 to 1.0 wt pct, due to the absence of oxygen source, namely, Al_2O_3 inclusions.

B. *Aluminum-Silicon Equilibrium Between Steel and Slag*

During the refining process, it is relatively easy for high-aluminum steel to take part in a reoxidation reaction with SiO_2 present in slag.[35–37]

$$4[Al] + 3(SiO_2)_{slag} = 3[Si] + 2(Al_2O_3)_{slag\ or\ inclusion}. \quad [6]$$

The following equation was derived from the study of Reference 25:

$$\log K_{Al-Si} = -6.94 + 37670/T. \quad [7]$$

Because MgO plays an important role in protecting the furnace lining, it is imperative that the appropriate

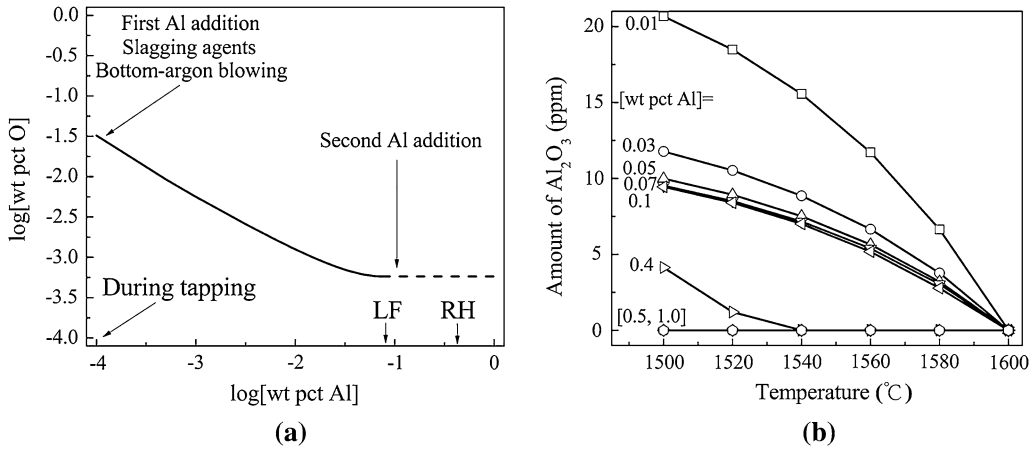

Fig. 2—(*a*) Assumed relationship between the dissolved [O] and [Al] in liquid steel at 1873 K (1600 °C). (*b*) Precipitation and amounts of Al_2O_3 from refining temperature up to close to liquidus temperature of steel. LF: ladle furnace; RH: vacuum degassing cycle refining furnace.

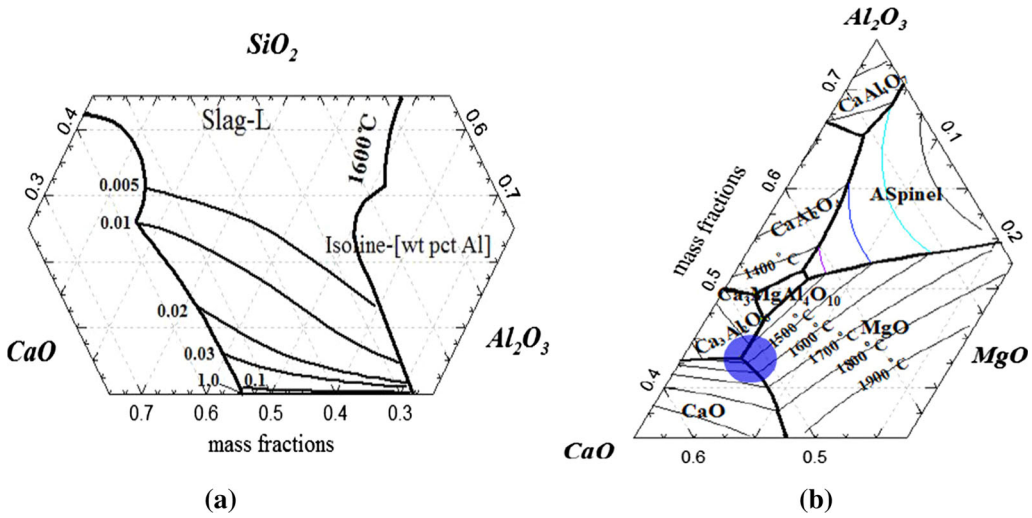

Fig. 3—(*a*) Equilibrium results between CaO-Al_2O_3-SiO_2-8 wt pct MgO and isolines of [wt pct Al] at 1873 K (1600 °C). Elements of steel except [Al] belong to 38CrMoAl shown in Table I. (*b*) Equilibrium phase diagram of CaO-Al_2O_3-MgO system.

amount of MgO should be present in the slag (assuming 8 wt pct). For CaO-Al_2O_3-SiO_2-8 wt pct MgO refining slag, the isolines of the mass fractions of dissolved [Al] at 1873 K (1600 °C) were calculated using FactSage according to Eq. [6] (Figure 3(a)). It is clear that it is impossible to inhibit the occurrence of Reaction [6] unless the content of SiO_2 in slag can be reduced to below 1.0 wt pct when the dissolved [Al]≥0.1 wt pct.

Therefore, the compositions of the final refining slag are designed in a region (light shadow area in Figure 3(b)) where the mass ratio CaO/Al_2O_3 (C/A) is ~1.2 to 1.5 and the SiO_2 content could be completely ignored, which demonstrated the benefits of preventing reoxidation of molten steel and absorbing the Al_2O_3 inclusions by reducing the activity of Al_2O_3 and the melting temperature of slag.[38] However, in the actual smelting process, the reaction of Eq. [6] cannot be inhibited completely, because a certain amount of SiO_2 in slag is unavoidable due to that SiO_2 content of the converter slag is high and raw slag materials may also introduce some SiO_2 into the ladle. Hence, in order to guarantee the effectiveness of Al_2O_3-inclusion control, the amount of converter tapping slag must be minimized, and the SiO_2 content in raw slag materials must be strictly restricted.

III. INDUSTRIAL TESTS

A. *Industrial Process Description*

To verify the effects of slag washing during tapping, accompanied with two-step Al-adding process on Al_2O_3 control for high-aluminum steel 38CrMoAl, we performed industrial tests under the production process presented in Figure 4. The typical target composition of this steel grades is shown in Table I.

During production, the deep desulphurization process of molten iron was accomplished at the stage of hot-metal pretreatment, and the resulfurization during the steelmaking and secondary refining processes was inhibited by strictly controlling the compositions and sulfur content of converter slag and refining slag. The RH was employed to lower [H] to ≤2 ppm, and the LF was used to make up the temperature losses of the RH process.

During tapping, a certain amount of SiO_2-minimized high-basicity slag (size 5 to 15 mm) (Table IV) and deoxidants were added to the ladle accompanied with bottom-argon blowing, according to the endpoint [O] of the converter and the necessary dissolved [Al] of steel. It should be noted that the necessary dissolved [Al] of steel after tapping was controlled at 0.08 to 0.12 wt pct to minimize the dissolved [O] content. For precisely controlling the refining slag composition within a reasonable range, the amounts of the primary deoxidization products generated, and high-basicity slag charged should be estimated with reasonable accuracy. To lower the melting point and facilitate the melting of high-basicity slag, a certain amount of fluorite was required. In view of the carry-over of converter slag after tapping, some Al-bearing modifier was added to the top slag in the ladle for reducing the FeO and MnO contents. The second addition of Al alloys was implemented at end of LF process to achieve ~1.0 wt pct dissolved [Al] of the steel. During the experiment, the steel and top-slag specimens were sampled (Figure 4).

B. *Analysis of Samples*

The compositions of the slag specimens were analyzed using an X-ray fluorescence spectrometer. The total oxygen and nitrogen contents [(T[O]) and ([N]), respectively] in the steel samples were determined using oxygen/nitrogen analyzer. The inclusions were detected and analyzed on the prepared steel samples using SEM-EDS to obtain the values of parameters such as morphology, size, and chemical composition.

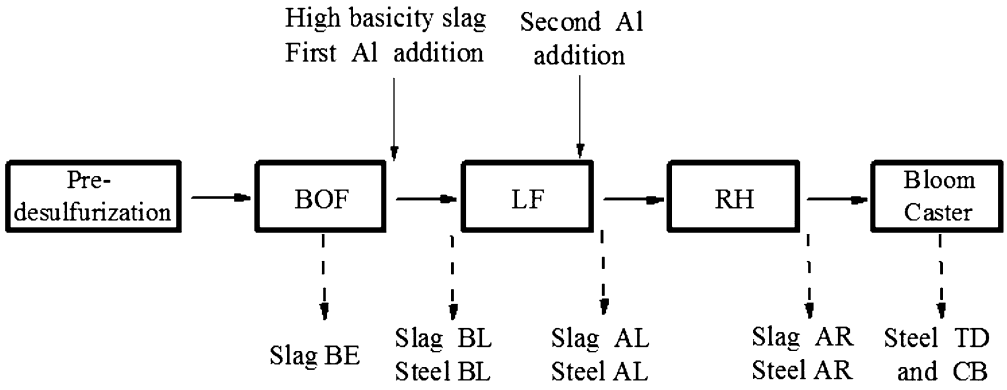

Fig. 4—Technical process used for producing 38CrMoAl steel and sampling locations. BOF: Basic oxygen furnace; BE: BOF Endpoint; BL: Before LF; AL: After LF; AR: After RH; TD: Tundish; CB: Casting Billet.

Table IV. Composition of High-Basicity Slag Charged During Tapping (Weight Percent)

CaO	Al_2O_3	SiO_2	MgO	CaF_2	*P*
≥70	≤5	≤5	≤6	≥6	≤0.10

IV. RESULTS AND DISCUSSION

A. *Castability of Molten Steel*

To reduce the reoxidation and guarantee the castability of steel, instruments such as sealing rings and processes such as stopper argon blowing and other comprehensive containment technology were used in the casting process. The casting conditions of five heats of steel were tracked. We found that the proposed process resulted in steady casting speeds and stopper opening positions, indicating that the casting conditions were controlled. Observation of the immersed nozzle after five heats of continuous casting (Figure 5) showed small amounts of oxides adhered to the nozzle wall. Thus, it would be feasible to extend to more than five heats of continuous casting by the slag washing during tapping, accompanied with two-step Al-adding process without calcium treatment.

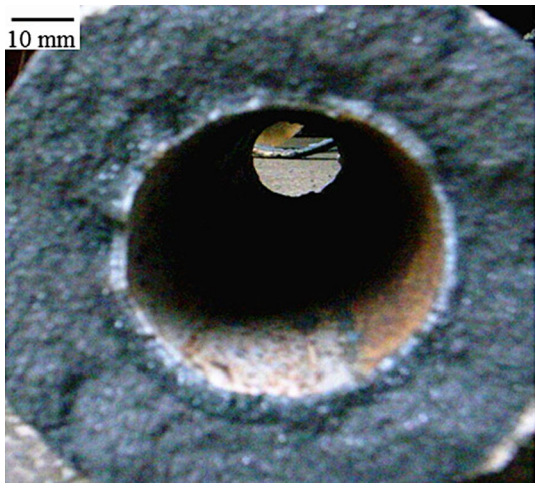

Fig. 5—Tundish nozzle after five heats of continuous casting steel.

B. *Slag Composition*

The change of top-slag composition of thirty-four heats with different locations is shown in Figure 6. As shown in Figure 6(a), ~10.0 wt pct SiO_2 was contained in converter final slag. After tapping, the SiO_2 concentration in the top slag decreased to ~5 wt pct as a result of dilution with SiO_2-minimized high-basicity slag charged during tapping, inclusions formed in deoxidization process, and some reduction of SiO_2 by dissolved [Al] in the steel. The SiO_2 content in refining slag dropped sharply to ~1.0 wt pct through LF treatment, which agrees with our calculated results (Figure 3(a)). The average mass C/A ratios (Figure 6(b)) in the top slags decreased from ~1.35 to ~1.25 by RH treatment. In addition, ~5.0 to 10.0 wt pct MgO and negligible amounts of impurities such as FeO, MnO, and P_2O_5 were also present in the top slags after LF and RH treatments. Clearly, both of the slags were basically located in the light shadow area, as shown in Figure 3(b).

C. *T[O] and [N]*

The T[O] and [N] of six heats at different locations are shown in Figure 7. It is evident that the average T[O] decreases gradually from 23.4 ppm before LF treatment to 17.7 ppm and 11.2 ppm after LF and RH treatments, respectively, to 9.6 ppm at tundish, and finally to 10.1 ppm in the casting bloom. In addition, the average [N] in steel decreased by vacuum degassing, while it increased slightly in the bloom.

It should be pointed that the T[O] in liquid steel after RH treatment was only ~11.2 ppm, and the actual dissolved [O] of course was much lower than this level. However, the theoretical values of dissolved [O] were calculated (using FactSage) as 13.9 to 14.3 ppm at

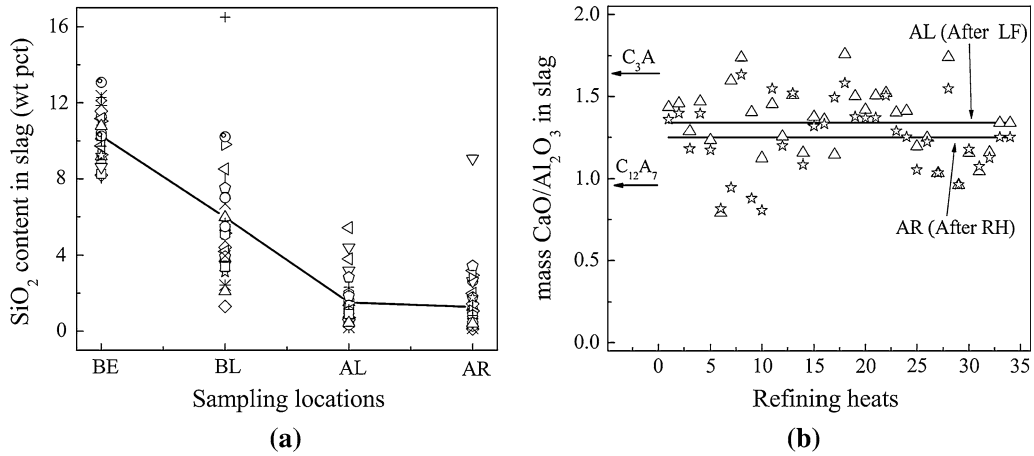

Fig. 6—Change of top slag composition at different sampling locations: (*a*) SiO_2 content in slag, where different symbols represent different heats; (*b*) mass ratios of C/A in slag, where the triangles indicate the heats after LF and stars indicate the heats after RH. Solid lines follow the mean result from each sample location.

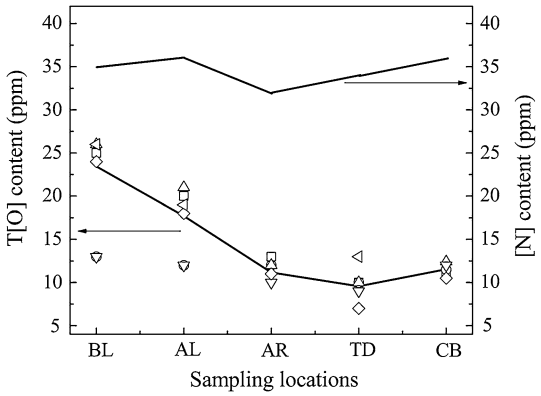

Fig. 7—T[O] and [N] of several heats at different sampling locations, where different symbols represent different heats. Solid lines follow the mean at each sampling point.

1873 K (1600 °C) by assuming that thermodynamic equilibrium were attained among slag, steel, and inclusions during RH treatment, where the mass C/A ratios in slag (7.5 wt pct MgO) were in 1.2 to 1.5 range. Obviously, the estimated values of dissolved [O] were much greater than the actual dissolved [O]. Therefore, it was reasonable to believe that the actual dissolved [O] did not increase but still remain at the minimum (~5.8 ppm) with further increasing dissolved [Al] from ~0.1 to 1.0 wt pct because of the absence of an oxygen source. One of the reasons was that dynamic condition of oxygen absorption was insufficient in steel covered by ladle slag. At the same time, after the second Al addition, the average T[O] reduced further from around 20 to 11.2 ppm (after RH treatment), which indicated that unlike the Al_2O_3, Ca-aluminate inclusions (which would be explained in the following text) might not be an oxygen source for dissolved [O] to increase when the dissolved [Al] further increased from ~0.1 to 1.0 wt pct; thus, the second reason was the modification and removal of primary Al_2O_3 inclusions.

D. *Effect of Slag Washing on Inclusion Control*

The morphology and size of typical inclusions observed in each steel sample are shown in Figure 8, where about forty to sixty oxide inclusions are analyzed for each sample. During BOF tapping, appropriate amount Al and high-basicity slag were added to the molten steel accompanied with bottom-argon blowing. Subsequently, globular shaped Ca-aluminates between $3CaO{\cdot}Al_2O_3$ (C_3A) and $12CaO{\cdot}7Al_2O_3$ ($C_{12}A_7$) with homogeneous composition were detected typically in liquid steel after tapping, and some of them contained very small amount of MgO (less than 3 wt pct) (Figure 8(BL1) to (BL3)), which might result from the following conditions:

(1) Direct reaction between high-basicity slag and Al_2O_3 inclusion during slag washing because of the good thermodynamic and dynamic conditions.[39,40]

$$y(CaO)_{slag} + x(Al_2O_3)_{inclusion} = y(CaO \cdot xAl_2O_3)_{liquid,\ inclusion\ or\ slag}. \quad [8]$$

It has been reported that the Gibbs free energy of the reaction of Eq. [8] showed significant negative values and they decreased by the order of $CaO{\cdot}Al_2O_3$ (CA), C_3A, and $C_{12}A_7$ within the steelmaking-temperature ranges, expressing that it was possible to form lower melting point Ca-aluminates from the perspective of the thermodynamics.[41,42] Lind *et al.*[10,39,43] investigated the mechanism and kinetics of reactions between solid CaO and Al_2O_3 in the absence of molten steel at 1873 K (1600 °C), proving that the chemical reaction between Al_2O_3 and CaO was the rate-controlling step; even then, solid CaO and Al_2O_3 could be completely liquidized to liquid Ca-aluminates within 2 to 3 min. Many investigations[44–49] have been carried out for the dissolution of Al_2O_3 in slag, demonstrating that the dissolution rate of Al_2O_3 particle decreased with increasing Al_2O_3 content in slag due to that the driving force of Al_2O_3 dissolution decreased. In

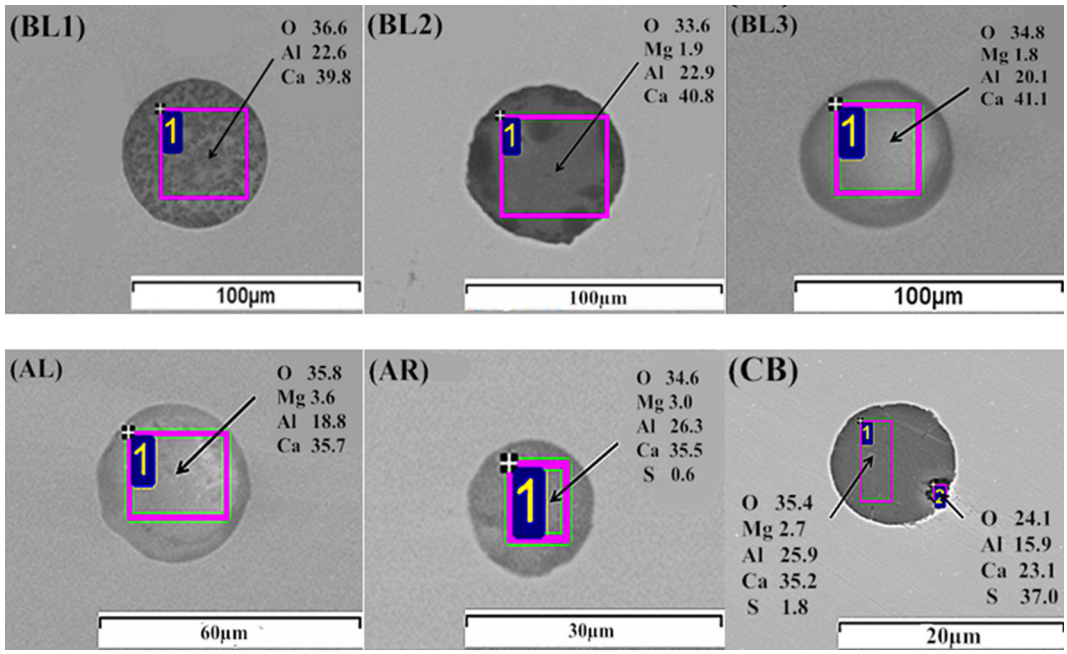

Fig. 8—Morphology and size of typical inclusions in steel. BL1-BL3: Before LF; AL: After LF; AR: After RH; CB: Casting billet.

addition, the addition of small amounts of MgO and CaF_2 could result in significant increase of the dissolution rate owing to that the viscosity of slag decreased so as to increase diffusion coefficient, while the existence of SiO_2 could lead to an opposite result.[49] Also, temperature had a greatly positive influence on Al_2O_3 dissolution.[48,49] And finally, the boundary layer diffusion inside the slag phase was the rate limiting step of the dissolution process, which was suggested.[44–47] Valdez *et al.*[50] also measured the dissolution kinetics of Al_2O_3 particle with 120 μ diameter in ladle slag by direct observation of the dissolution process through the confocal scanning laser microscope and found that the inclusion dissolution time in slag was only dozens of seconds but was significantly longer than the separation times of Al_2O_3 at the interface (<5 seconds). Therefore, as long as slag chemistries are designed to avoid saturation, large Al_2O_3 particle should easily be absorbed. Obviously, the slag used during tapping in present study, which has high CaO content, some MgO and CaF_2 contents, and low SiO_2 and Al_2O_3 contents (Table IV), was very fit for the dissolution of Al_2O_3 inclusion. At the same time, the boundary layer diffusion inside the slag phase as the rate-controlling step could not be a big problem because perfect dynamic conditions could be produced by slag washing during tapping.[34]

(2) MgO and CaO in high-basicity slag could be simultaneously reduced by dissolved [Al] to supply dissolved [Mg] and [Ca] into the molten steel.[4,51,52]

$$3(MgO)_{slag} + 2[Al] = (Al_2O_3)_{slag} + 3[Mg]. \quad [9]$$

The equilibrium constant of the above reaction was obtained by the combination of the studies.[25,53]

$$\log K_{Al-Mg} = -33.41 + 49900/T, \quad [10]$$

$$3(CaO)_{slag} + 2[Al] = (Al_2O_3)_{slag} + 3[Ca]. \quad [11]$$

The following equation was derived from the studies of references.[25,54]

$$\log K_{Al-Ca} = -30.44 + 42340/T. \quad [12]$$

Thus, Al_2O_3 inclusions, which formed as soon as aluminum was added to molten steel, were reacted with dissolved [Mg] due to its higher activity than dissolved [Ca] in the melt, leading to the formation of $MgO{\cdot}Al_2O_3$ (MA) inclusions.[4,51]

$$4(Al_2O_3)_{inclusion} + 3[Mg] = 3(MgO{\cdot}Al_2O_3)_{inclusion} + 2[Al]. \quad [13]$$

The equilibrium constant of the above reaction was obtained from the literature.[25,53,55]

$$\log K_{Mg-Al} = 34.37 - 46950/T. \quad [14]$$

The isolines of $a_{[Mg]}$ and $a_{[Ca]}$ between CaO-Al_2O_3-MgO slag and steel at 1873 K (1600 °C) were calculated using FactSage on the basis of Eqs. [9] and [11] (Figure 9), where the dissolved [Al] after slag washing was assumed at 0.1 wt pct. The refining slag compositions are shown as a shadow area on the phase diagram, where the SiO_2 content in the topslag is ignored because only 1.0 wt pct SiO_2 could be rested at equilibrium. As can be seen, the equilibrium values of $a_{[Mg]}$ and $a_{[Ca]}$ are ~50 × 10^{-4} and ~23 × 10^{-4}, respectively. A recent study conducted by Fujii *et al.*[56] revealed the variation of

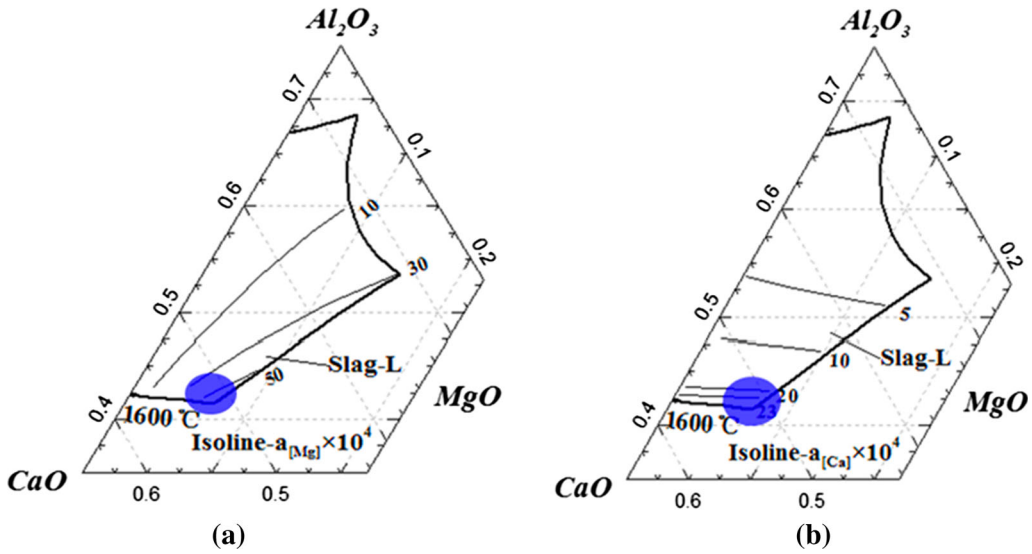

Fig. 9—Equilibrium results between CaO-Al_2O_3-MgO slag and isolines of (*a*): $a_{[Mg]}$; and (*b*): $a_{[Ca]}$ at 1873 K (1600 °C). Elements of steel except [Al] ([Al] = 0.1 wt pct) belong to 38CrMoAl shown in Table I.

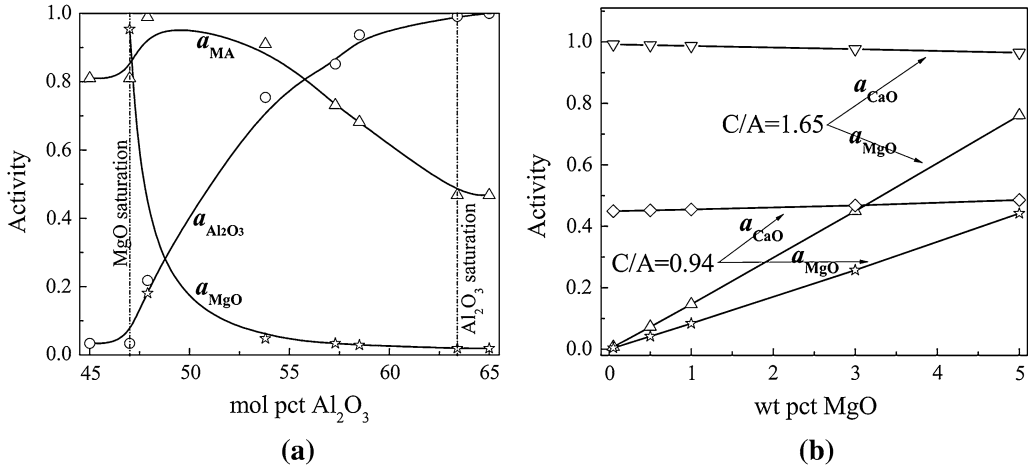

Fig. 10—(*a*) Activities of MgO, Al_2O_3,and MA in the spinel solid solution at 1873 K (1600 °C)[56]; (*b*) Activities of CaO and MgO in Ca-aluminates calculated using FactSage 6.3 at 1873 K (1600 °C).

activity of MA in the solid solution region (Figure 10(a)) as a function of composition. In Eq. [13], the activity of MA was taken as 0.47 while that of Al_2O_3 was taken as unity because of the negligibly small solubility of MgO into Al_2O_3. Thus, the Gibbs free energy for Eq. [13] was estimated to be −193.06 kJ/mol, indicating that MA could form easily. However, the formed MA was not stable and could be changed to CaO-Al_2O_3-MgO when dissolved [Ca] entered the steel.[51,52]

$$(\mathrm{MgO})_{\text{in MgO}-\mathrm{Al_2O_3}} + [\mathrm{Ca}] = (\mathrm{CaO})_{\text{in CaO}-\mathrm{Al_2O_3}-\mathrm{MgO}} + [\mathrm{Mg}]. \quad [15]$$

The equilibrium constant was obtained from the combination of references.[53,54]

$$\log K_{\mathrm{Ca-Mg}} = -0.99 + 2520/T. \quad [16]$$

In Eq. [15], the activity of MgO was taken as 0.45 for C_3A and 0.26 for $C_{12}A_7$ because of the small content of MgO (assuming 3 wt pct) in the Ca-aluminates observed immediately after slag washing, and the activity of CaO in C_3A as 0.98 and that of $C_{12}A_7$ as 0.47 (Figure 10(b)). Consequently, the Gibbs free energy for Eq. [15] was estimated as 11.47 kJ/mol for C_3A and 8.57 kJ/mol for $C_{12}A_7$, showing that the MA could not be modified to C_3A or $C_{12}A_7$ inclusions with MgO content less than 3 wt pct by the indirect supply of dissolved [Ca] *via* slag.

Therefore, it could be speculated that only the direct reaction between SiO_2-minimized high-basicity slag and Al_2O_3 (case 1 above) could be the reason for the formation of Ca-aluminates observed immediately after slag washing in the process of high-aluminum steel.

As shown in Figure 8(AL) to (AR), compared with the Ca-aluminates after slag washing, the MgO content in inclusions obtained though the LF and RH treatments increased a little, possibly due to that some

dissolved [Mg] in liquid steel, which came from the reduction of MgO in slag by dissolved [Al], entered into the inclusions.[4,51] However, much detailed work was still needed to quantitatively discuss. In casting billet sample, some Ca-aluminates associated with CaS were detected, owing to the decrease of solubilities of dissolved [Ca] and [S] in Ca-aluminates during the cooling of steel.[8] Consequently, though the adoption of above proposed methodology, not only the primary Al_2O_3 formed during tapping can be modified and removed mostly, but also the precipitation of second Al_2O_3 during cooling from the deoxidation temperature to the liquidus temperature can be avoided. As a result of these benefits, the desired continuous castability of high-aluminum steel is achieved.

V. CONCLUSIONS

The thermodynamics between aluminum and oxygen in liquid steel with high-aluminum content as well as slag and steel equilibrium was investigated. And the effect of the slag washing during tapping, accompanied with two-step Al-adding process and appropriate top-slag refining process on inclusion control in the process of 38CrMoAl steel production, was studied, and the following conclusions were drawn:

1. Thermodynamic calculations indicate that for high-aluminum steel with 1.0 wt pct dissolved [Al], the Al_2O_3 inclusion may not precipitate during cooling from deoxidation temperature to the liquidus temperature, if the actual dissolved [O] can be kept from increasing when the dissolved [Al] further increases from 0.1 to 1.0 wt pct.
2. Strong chemical reaction happened between liquid steel and slag, and SiO_2 content in top slag was reduced to only ~1.0 wt pct during the refining process of high-aluminum steel.
3. Low-melting point Ca-aluminates after slag washing were observed typically, and MgO content in these Ca-aluminates after the LF and RH treatments increased a little.
4. Industrial tests show that there was no nozzle clogging occurred for five heats of continuous casting without Ca treatment.

REFERENCES

1. H. Todoroki and N. Shiga: *Proceedings 4th Int.ernational Congress on Science and Technology of Steelmaking*, Gifu, Japan, 2008, Iron and Steel Institute of Japan, Tokyo, Japan, 2008, pp. 121–24.
2. C.E. Cicutti, J. Madias, and J.C. Gonzalez: *Ironmaking Steelmaking*, 1997, vol. 24 (2), pp. 155–59.
3. K. Sakata: *ISIJ Int*., 2006, vol. 46 (12), pp. 1795–99.
4. J.H. Park and H. Todoroki: *ISIJ Int*., 2010, vol. 50 (10), pp. 1333–46.
5. J.B. Jeffrey, A.M. Maureen, and T.N. Thinium: *Iron and Steel Technology Conference Proceedings*, Charlotte, North Carolina, 2005, Association for Iron and Steel Technology, Warrendale, Pennsylvania, 2005, pp. 99-106.
6. S. Stuart, J. Keegan, and M. Nicole: *Iron Steel Technol*., 2008, vol. 5 (7), pp. 38–49.
7. D. Janke, Z.T. Ma, P. Valentin, and A. Heinen: *ISIJ Int*., 2000, vol. 40 (1), pp. 31–39.
8. S. Abdelaziz, G. Megahed, I. El-Mahallawi, and H. Ahmed: *Ironmaking Steelmaking*, 2009, vol. 36 (6), pp. 432–41.
9. N. Verma, P.C. Pistorius, R.J. Fruehan, M. Potter, M. Lind, and S. Story: *Metall. Mater. Trans. B*, 2011, vol. 42B, pp. 711–19.
10. M. Lind and L. Holappa: *Metall. Mater. Trans. B*, 2010, vol. 41B, pp. 359–66.
11. K. Ahlborg: *84th Steelmaking Conferene Proceedings*, Baltimore, Maryland, 2001, Iron and Steel Society, Warrendale, Pennsylvania, 2001, pp. 861–70.
12. C.J. Zhang, K.K. Cai, and W.X. Yuan: *Iron Steel*, 2006, vol. 41 (8), pp. 31–33.
13. K.K. Cai: *Quality Control of Continuous Casting Slab*, Metallurgical Industry Press, Beijing, 2010, pp. 54.
14. G.G. Mikhailov and L.A. Chernova: *Russian Metallurgy (Metally)*, 2008, vol. 2008(8), pp. 727–29.
15. E.T. Turkdogan: *Proceedings of 1st International Calcium Treatment Symposium*, University of Strathclyde, Glasgow, Scotland, 1988, The Institute of Metals, London, 1988, pp. 3–13.
16. D.D.-Z. Lu: Doctor of Philosophy, Thesis, McMaster University, 1992.
17. G.J.W. Kor and P.C. Glaws: *Fundamentals of Iron and Steelmaking*, 11th ed., AISE Steel Foundation, London, Isle of Man, 1998, pp. 661-13.
18. C. Espinosa: Master Thesis, University of Buenos Aires, 2005.
19. S.K. Choudhary and A. Ghosh: *ISIJ Int*., 2008, vol. 48 (11), pp. 1552–59.
20. L.H. Mh, M. Liukkonen, and M. Lind: *Ironmaking Steelmaking*, 2003, vol. 30 (2), pp. 111–15.
21. K. Rackers and B.G. Thomas: *Proceedings of 78th Steelmaking Conference*, Nashville, Tennesse, 1995, Iron and Steel Society, Warrendale, Pennsylvania, 1995, vol. 78, pp. 723–34.
22. J.M.A. Geldenhuis and P.C. Pistorius: *Ironmaking Steelmaking*, 2000, vol. 27 (6), pp. 442–449.
23. G.J. Kor: *Proceedings of Elliott Symposium*, Cambridge, Massachusetts, 1990, Iron and Steel Society, Warrendale, Pennsylvania, 1990, pp. 400–17.
24. K. Larsen and R.J. Fruehan: *Iron Steelmaker*, 1990, vol. 17, pp. 45–52.
25. Steelmaking Data Sourcebook: *The Japan Society for the Promotion of Science, the 19th Committee on Steelmaking*, Gordon and Breach Science Publications, New York, NY, 1988.
26. X. H. Huang: *Ferrous Metallurgical Principle*, 3th edn., Metallurgical Industry Press, Beijing, 2008, pp. 111.
27. G.K. Sigworth and J.F. Elliott: *Met. Sci*., 1974, vol. 8 (9), pp. 298–310.
28. H. Itoh, M. Hino, and S. Ban-ya: *Metall. Mater. Trans. B*, 1997, vol. 28B, pp. 953–56.
29. R.J. Fruehan: *Metall. Trans*., 1970, vol. 1, pp. 3403–10.
30. J.D. Seo, S.H. Kim, and K.R. Lee: *Steel Res*., 1998, vol. 69 (2), pp. 49–53.
31. D. Janke and W.A. Fisher: *Arch. Eisenhüttenwes*., 1976, vol. 47, pp. 195–98.
32. S. Dimitrov, A. Weyl, and D. Janke: *Steel Res*., 1995, vol. 66 (1), pp. 3–7.
33. I.H. Jung, S.A. Decterov, and A.D. Pelton: *Metall. Mater. Trans. B*, 2004, vol. 35B, pp. 493–507.
34. E.T. Turkdogan, R.S. Bogan and S. Gilbert: *Proceedings of 74th Steelmaking Conference*, Washington, 1991, Iron and Steel Society, Warrendale, Pennsylvania, 1991, pp. 423–34.
35. S. Maeda, T. Soejima, T. Saito, H. Matsumoto, H. Fujimoto and T. Mimura: *Proceedings of 72th Steelmaking Conference*, Chicago, Illinois, 1989, Iron and Steel Society, Warrendale, Pennsylvania, 1989, pp. 379–85.
36. J.F. Elliott, M. Gleiser and V. Ramakrishna: *Thermochemistry for Steelmaking*, vol. 2, Addison-Wesley Publishing Company, London, Isle of Man, 1963, pp. 22.
37. S.W. Cho and H. Suito: *ISIJ Int*., 1994, vol. 34 (2), pp. 177–85.
38. B.H. Yoon, K.H. Heo, J.S. Kim, and H.S. Sohn: *Ironmaking Steelmaking*, 2002, vol. 29 (3), pp. 215–18.
39. Z.J. Han, L. Liu, M. Lind, and L. Holappa: *Acta Metall. Sin. (Engl. Lett.)*, 2006, vol. 19 (1), pp. l–8.

40. M. Lind: Doctor of Philosophy, Helsinki University of Technology, 2006.
41. S. Saxena, T. Engh, and S. Pednukan: *Scand. J. Metall.*, 1975, vol. 4, pp. 42–48.
42. N.K. Das, N. Sen, M. Ghosh, and R. Sau: *Scand. J. Metall.*, 2005, vol. 34, pp. 276–82.
43. Z. Han, M. Lind, and L. Holappa: *International Conference on Non-metallic Inclusions Control and Continuous Improvement of Processes based on Objective Measurement*, Borlänge, Sweden, 2004, Jernkontoret, 2004, pp. 1–18.
44. S. Taira, K. Nakashima, and K. Mori: *ISIJ Int.*, 1993, vol. 33 (1), pp. 116–23.
45. J.-Y. Choi, H.G. Lee, and J.-S. Kim: *ISIJ Int.*, 2002, vol. 42 (8), pp. 852–60.
46. K. Ogawa, K. Inoue, S. Koyama, M. Shimotsusa, and Y. Fukuzaki: *Proceedings of 4th International Conference on Molten Slags and Fluxes, Sendai*, Japan, 1992, Iron and Steel Institute of Japan, Tokyo, Japan, 1992, pp. 336–39.
47. K. Shinme and T. Matsuo: *Proceedings of 4th International Conference on Molten Slags and Fluxes*, Sendai, Japan, 1992, Iron and Steel Institute of Japan, Tokyo, Japan, 1992, pp. 336–39.
48. C. Tse, S.H. Lee, S. Sridhar, and A.W. Cramb: *Proceedings of 83th Steelmaking Conference*, Pittsburgh, Pennsylvania, 2000, Iron and Steel Society, Warrendale, Pennsylvania, 2000, pp. 219–29.
49. W.D. Cho and P. Fan: *ISIJ Int.*, 2004, vol. 44 (2), pp. 229–34.
50. M. Valdez, K. Prapakorn, S. Shidhar, and A.W. Cramb: *Iron and Steel Society Technology Conference Proceedings*, Indianapolis, Indiana, 2003, Iron and Steel Society, Warrendale, Pennsylvania, 2003, pp. 789–98.
51. M. Jiang, X.H. Wang, B. Chen, and W.J. Wang: *ISIJ Int.*, 2010, vol. 50 (1), pp. 95–104.
52. J. Yang, W.J. Wang, M. Jiang, and X.H. Wang: *J. Iron. Steel Res. Int.*, 2011, vol. 18 (7), pp. 8–14.
53. H. Itoh, M. Hino, and S. Ban-ya: *Tetsu-to-Hagané*, 1997, vol. 83 (10), pp. 623–28.
54. H. Itoh, M. Hino, and S. Ban-ya: *Tetsu-to-Hagané*, 1997, vol. 83 (11), pp. 695–700.
55. H.R. Rein and J. Chipman: *Trans. Metall. Soc. AIME*, 1965, vol. 233, pp. 415–25.
56. K. Fujii, T. Nagasaka, and M. Hino: *ISIJ Int.*, 2000, vol. 40 (11), pp. 1059–66.